SELECTIVE MOVEMENTS OF SAND AND GRAVELS AND RESULTING DYNAMIC MORPHOLOGY CHANGES OBSERVED AROUND THE TENRYU RIVER MOUTH

YOSHIMITSU TAJIMA, HIJIANG LIU, TOMOHIRO TAKAGAWA, SHINJI SATO

Department of Civil Engineering, The University of Tokyo, Hongo 7-3-1, Bunkyo-ku, Tokyo 113-8656, Japan. yoshitaji@coastal.t.u-tokyo.ac.jp.

Abstract: This study focuses on the selective movements of sand grains and gravels around the sand spit of the Tenryu River mouth in Japan. Color sand and gravels were placed at the outer edge of the swash zone of both west and east sides of the sand spit and their changing spatial distributions were traced afterward. Observed different movements of sand and gravels were compared with the dynamic deformation of the sand spit and surrounding hydrodynamic characteristics such as waves and currents, all of which were continuously and quantitatively analyzed based on succeeding snap shot images recorded by field cameras and X-banded radar. Numerical model based on Boussinesq-type non-linear dispersive wave with porous layer was finally applied to further investigate the hydrodynamic characteristics observed around the river mouth where waves, currents and complex river mouth morphology interact with each other.

Introduction

Morphology of a sand spit, developed at the river mouth, has significant impact on surrounding hydrodynamic characteristics such as waves, currents, and resulting sediment transport. Due to such dynamic and active movement of the bottom sediments, it is virtually difficult especially around the river mouth to install ordinary measuring devices such as velocity meter and wave gauges to quantitatively capture such interactive features of hydrodynamics and morphology deformations. Remote sensing techniques, instead, are often applied to monitor physical processes around the surf zone and river mouth (e.g., Lippmann and Holman, 1989; Greidanus, 1997; and Bell, 1999). Authors installed field cameras and X-band radar around the Tenryu river mouth in Japan and successfully captured various dynamic processes such as collapse and redevelopment of the sand spit under the flood, stormy waves, and the following moderate waves (e.g., Liu et al., 2008 and Tajima et al., 2009). While these field observations clarified various features of sand spit deformations, such as alongshore extension of the spit under the moderate waves and cross-shore movement of the spit during either flood or stormy waves, it is not yet clear about the detailed physical mechanisms of such deformation processes possibly due to the lack of field data. This study therefore focuses on the actual movement of sand and gravels on the sand spit, which should directly characterize the spit deformation, through unique sets of field survey using color sand and gravels as tracers.

Field Survey

Continuous field surveys had been carried out around the Tenryu river mouth through the year of 2009. This study focuses on the period from July to October during which dynamic morphology change was observed around the sand spit due to severe stormy waves and relatively large river discharge. Figure 1 shows the plane view of the Tenryu river mouth with spatial allocations of newly installed field cameras and an X-band radar. Field cameras recorded the succeeding snap shot images of the Tenryu river mouth with time intervals of 1.2 seconds whereas the X-band radar recorded the spatial distributions of the intensity of the reflected signals with time intervals of 2 seconds. Besides these continuous remote sensing data, we also carried out topographic measurements of the sand spit for seven times during the focusing survey period.

In order to investigate the actual movements of the sediments on the sand spit, this study also carried out the following tracing survey of color sands and gravels. As shown in the Figure 1, color sands and gravels were placed in the swash zones of both west and east sides of the spit at 7:00 on July 28, 2009 and their movements were traced. Diameters of the color sand and gravels respectively range from 0.2mm to 0.4mm and 1 cm to 3 cm and the amount of each color sand and gravels placed at each site was 250kg. Movement of color sands and gravels were then traced by the following procedures. About 100g of sediments on the ground within the 1-cm-thick surface layer was sampled and the number of color sand included in the sample was counted by a device which

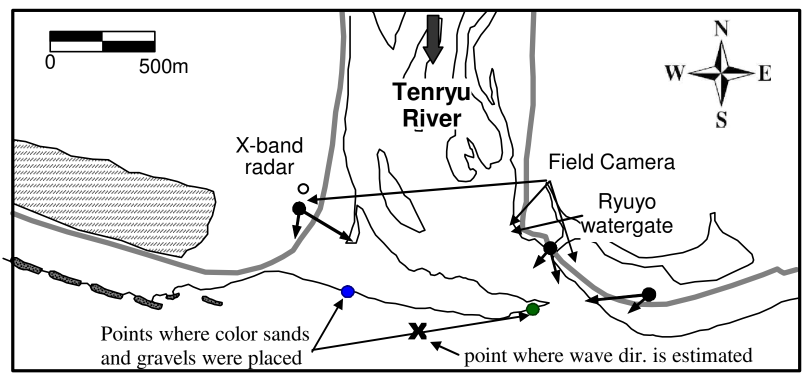

Fig.1 Plane view of the Tenryu river and field survey setups

automatically detects the color sand based on a number of digital images of the sampled sand surface (Niu et al., 2009). The amount of color sand contained in each sample collected at different locations was then expressed in terms of ppm. On the west side of the sand spit, sampling locations were selected along the shoreline and about 1 meter landward from the highest upper edge of the swash zone at each sampling time. Since the ground level was relatively low around the east end of the sand spit and therefore overtopping wave appeared to transport sediments over the entire sand spit, sampling locations around the east tip of the spit were selected on the square grids with spatial intervals of 10 meters. Since the number of gravels were much less than the color sand grains, tracer gravels were directly searched by eyes at the site and the number of tracer gravels within a unit surface area was counted at the locations where the gravels were found.

Hydrodynamic characteristics during the field survey were analyzed based on the images of field cameras and X-band radar. Besides these image-based information, we also used the following quantitative hydrodynamic data recorded by respective measuring instruments: (i) river discharge estimated from the water level data measured about 25km upstream from the Tenryu river mouth; (ii) wave heights, periods and directions recorded at the Ryuyo wave gauge, about 1000m offshore from the river mouth with water depth of 40m; and (iii) tidal water levels recorded at three different locations, i.e., at Kaketsuka, about 3km upstream from the river mouth, at Ryuyo water gate, just behind the river mouth, and at the Ryuyo wave gauge.

Deformation of the Sand Spit

Figure 2 shows the spatial deformation of the entire sand spit, in which shoreline locations were recorded by a portable differential GPS device. As seen in the figure, active deformation is observed mainly around the sea (south) side and east end of the sand spit. Exceptionally significant deformation was observed even around the land side (northside) of the spit from October 5th to 12th, during which the typhoon T1018 hit the pacific coast of Japan and caused severe stormy waves with significant wave height of 10 meters. From August 16th to September 24th, it is observed seaward and landward movement of the shorelines respectively around the west side and east side of the sand spit. This deformation somehow indicates significant westward littoral sediment transport during this period.

Quantification of the Spit Deformation

As seen in Figure 2, active morphology change was observed especially around the east tip of the sand spit. In order to investigate the more detailed characteristics of such dynamic deformation around the east end of the sand spit, this study utilized succeeding digital snap shot images recorded by a field camera. To avoid the influence of the tide level on the estimation of the shoreline locations, we first selected images when the time-averaged water level at the Ryuyo water gate was at TP+0.0m. Since the Ryuyo water gate is located just inside the river mouth, measured water level should already account for various factors such as tides, river flow and wave setup. Fifty succeeding images with 1.2-second time intervals were then used to reproduce "1-minute-averaged image," which was then used to determine the time-averaged shoreline locations. Finally, obtained time-averaged images were rectified to yield the images based on the geographic XY-coordinate system. This study applied Tajima et al.'s (2009) rectification technique which, introducing weight functions, improves the accuracy of the estimation of the XY coordinates in the far-camera field. Figure 3 shows an example of the original and rectified images around the east end of the sand spit. Based on 107 similar rectified images around the east end of the

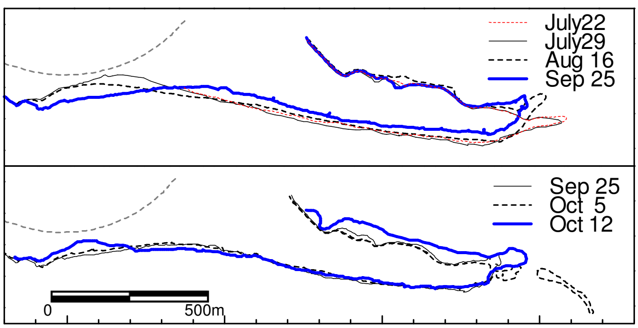

Fig.2 Spatial profiles of the sand spit at different time measured by GPS.

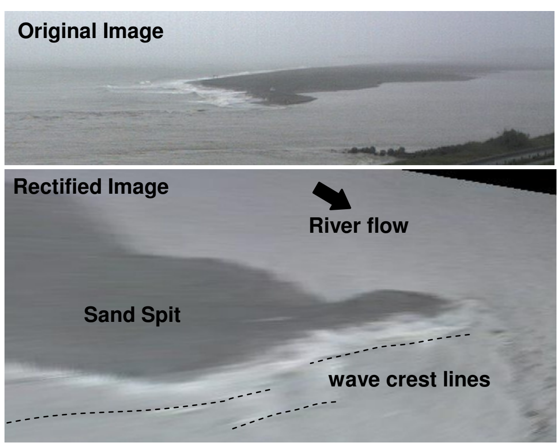

Fig.3 Examples of original and rectified images

sand spit, time-averaged shoreline profiles were extracted and compared with each other on the same XY coordinate system (Figure 4). Four digit numbers in the figure indicate the date when the images were recorded. For example, 1002 indicates October 2nd in 2009. As seen in the figure, shorelines are dynamically changing within a daily time scale. In order to quantitatively investigate the characteristics of the spit deformation, furthermore, this study divided the focusing area in north and south or in east and west rectangular domains, respectively, and compared the time-varying surface ground areas in each rectangular domain. Figure 4 shows the straight boundary lines which separate the area into north and south, and in east and west. Obtained time-series of the ground area are then directly compared with surrounding hydrodynamics such as waves, river discharge, and tides. Figure 5 shows the time-series of the estimated ground areas in each domain and surrounding various hydrodynamics. In the figure, wave directions were estimated at the surf zone in front of the sand spit, which should show stronger correlations with the observed sand spit deformations. Time-series of the images recorded by the X-band radar was applied to estimate the wave directions. At the location specified in Figure 1, instantaneous velocity components of the moving wave crest lines in the northward and eastward directions were first estimated from two succeeding images. Obtained time-series of the instantaneous wave directions were averaged over 10 minutes to get averaged velocity components which eventually yield the time-averaged wave directions. Figure 6 shows an example of the “snap shot” image recorded by X-band radar. As seen in the figure, wave crest lines are clearly observed in the nearshore area where wave directions were estimated.

Relationship between Spit Deformation and Surrounding Hydrodynamics

Based on Figures from 2 to 6, this section discusses the relationship between observed sand spit deformations and surrounding hydrodynamics.

Relatively large river discharge was observed around July 27th and, within a few days after July 27th, the tip of the spit was clearly eroded. The affected area, however, is limited only around the tip of the spit and the change of the estimated ground surface area was relatively small compared to the other period.

On August 9th, the typhoon T1009 caused relatively large waves with significant wave heights of 2.5m propagating from SSW and largely decreased the ground surface area in the domain S and vice-versa in the domain N. Accounting for the fact that the change of the ground surface area in domains E and W were relatively small, it is deduced that the cross-shore northward sediment movement was predominant compared to the alongshore movement during this period.

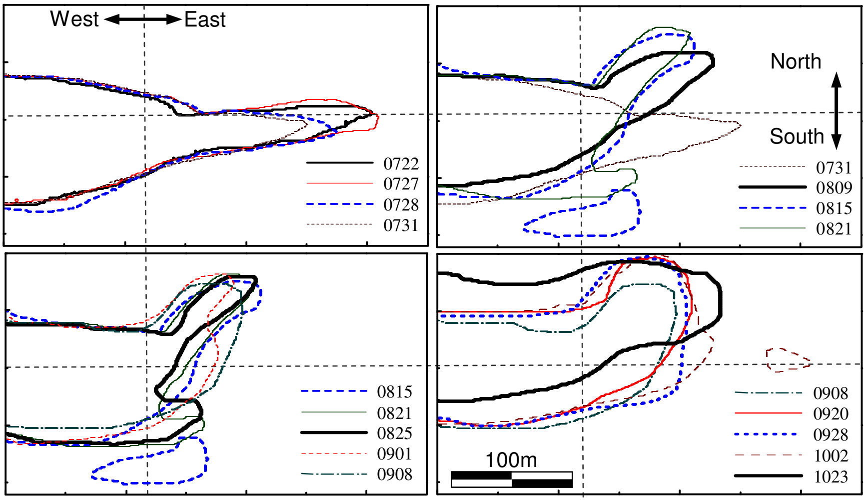

Fig.4 Time-varying profiles of the east tip of sand spit and Tenryu river and field survey setups

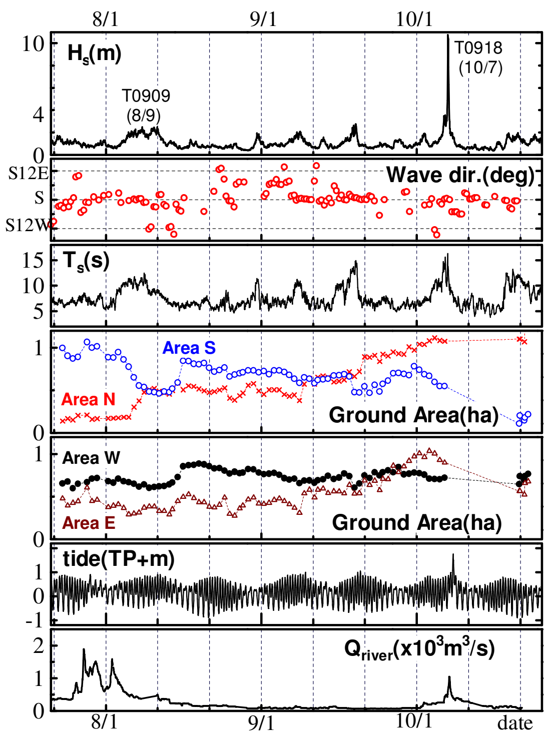

Fig.5 Time-series of various hydrodynamics and ground area in north, south, east and west area.

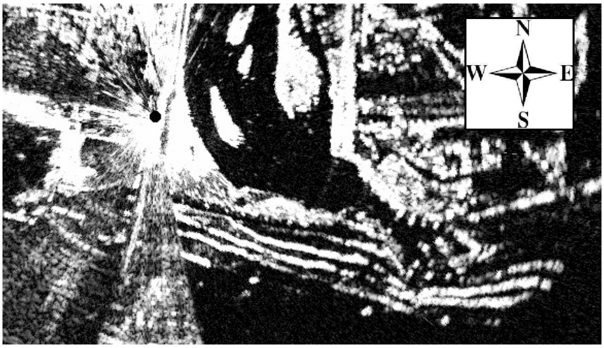

Fig. 6 Example of a “snap shot” image recorded by X band radar (2:00, Aug. 8, 2009)

Milder waves after the storm increased the ground surface area around the sea side within a relatively short period of time. Since this increase is observed both in the east and west regions, this increase of the ground surface was deduced mainly due to wave-induced onshore movement of the sediments which had been transported seaward and deposited during the stormy waves.

From the middle of August to the beginning of September, wave directions turned from SSW to SSE and this change of the wave directions surely supports the westward sediment transport deduced from the shoreline changes observed in Figure 2. While the clear evidence of the westward sediment movement was observed around the central and western part of the sand spit, east end of the sand spit was relatively stable and the relatively small changes of the ground surface area observed in the area E appears to have stronger correlations with spring tides or with wave period rather than the wave heights. This observed feature somehow indicates that east end of the spit has little westward sediment transport and this lower ground area was rather affected by overtopping waves which were predominant especially during the high tide. After the middle of September, relatively mild waves continued but their directions again turned slightly from west side and gradually increased the ground surface area in the domains, E and N.

Finally, the typhoon T1018 hit the area on October 7th and caused severe stormy waves with significant wave heights of 10 meters. Wave overtopping, observed on the entire sand spit, moved the entire sand spit in the landward direction. According to Takagawa et al. (2011), alongshore distributions of the estimated amount of the northward sediment transport during the storm showed fairly strong correlation with the alongshore distributions of the highest ground level on the spit. These observed facts also indicate that the characteristics of the sand spit deformation are highly affected by overtopping waves.

Investigation of Selective Movement of Sand and Gravels

Figures 7 and 8 respectively show spatial distributions of the collected color sands and gravels at different sampling times. The amount of the collected color sand is expressed in terms of parts per million while the amount of tracer gravels is expressed in terms of the actual number of gravels out of the unit ground surface area of square meters. As shown in Figure 8, the tracer gravels were initially placed along the line parallel to the shoreline with finite length of 30m whereas color sands were placed at the points on east and west sides of the spit, respectively.

As observed in Figure 7, all the blue color sands placed on the west side of the spit moved westward and their moving distance abruptly increases after 10 am when the tide level reached to its daily peak. While the increase of the tidal water level from 7am to 10 am was just about 30cm, movement of the color sand placed at the outer edge of the swash zone showed clear correlation with tide. While the movement of the gravels were less active compared to the color blue sand, their moving direction was also in the westward direction. Spatial distributions of the wave crest lines recorded by the X-band radar clearly showed the nearshore waves propagating from SSE and the estimated averaged wave direction at the Ryuyo wave gauge was S12^{o}E. The angle of the shoreline was 17 degrees in the clockwise direction from the east-west line and therefore the

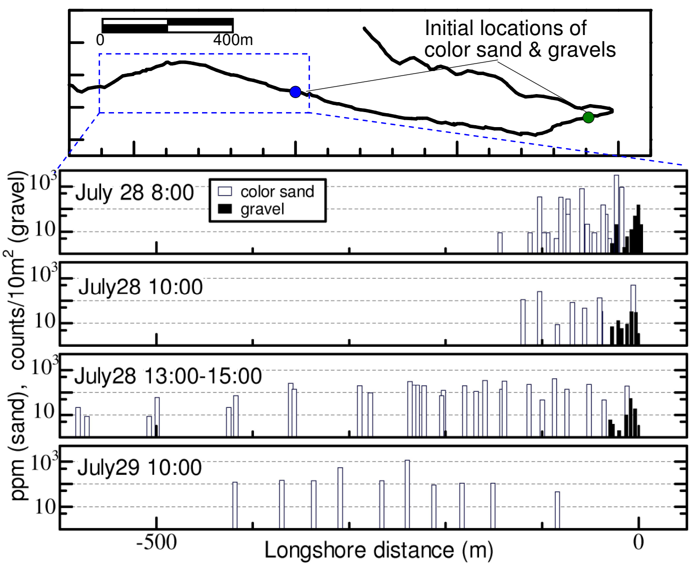

Fig. 7 Alongshore distributions of color sands and tracer gravels placed at the west side of the spit.

expected westward littoral sediment transport is also consistent with the observed movement of the blue sands and gravels.

In contrast to the blue sands and tracer gravels placed on the west side of the spit, the green sands and tracer gravels, placed in the east end of the spit, moved eastward as shown in Figure 8. In Figure 8, a part of the ground area within 20-meter from the east end of the spit was the place where the ground level was low and frequent overtopping waves did not allow us to collect surface sand samples. Instead, locations where no color sand was found in the collected samples were indicated as solid circles in the figure. Difference between sands and gravels were also clearly observed. While both sand and gravels moved in the north-eastward direction, gravels tended to move more toward the north. Furthermore, northward movement of the gravels appeared to be enhanced at 13:00 on the 29th after the placed gravels experienced the first high tide at 22:00 on the 28th. These features will be discussed later with numerical analysis of the hydrodynamic characteristics around the sand spit. Observed northward movement of sands and gravels surely corresponds to the northward deformation of the sand spit discussed in the previous section.

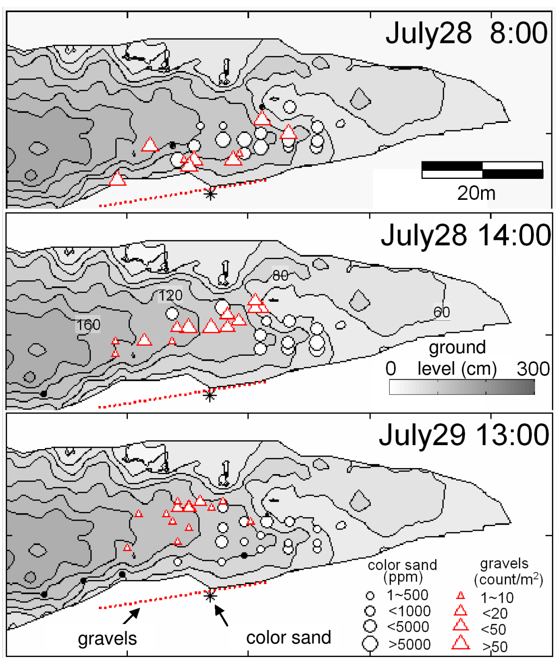

Fig.8 Spatial distributions of color sand and gravels placed at the east tip of the spit.

Hydrodynamics around the Sand Spit

This section further investigates the hydrodynamic characteristics around the sand spit based on recorded digital images and numerical analysis. Following the observations and discussions about the spit deformations and selective movements of sand and gravels, this section focuses on wave overtopping and the alongshore distributions of the angle between the wave and the shore-normal directions, which, as seen in well-known CERC formula, should determine the alongshore directions of the sediment movements.

This study applied Tajima et al.'s (2006) Boussinesq-type weak non-linear dispersive wave model for computations of wave-current interacting fields including wave run-up around the swash zone. The model followed the concept of Madsen et al.'s (1997) porous layer model, which enables efficient computation of the wave run-up in the swash zone. Applicability of the model was verified through the comparisons with the experimental data in which periodic waves were normally incident on a plane sloping beach with a submerged breakwater placed around the surf zone. The model was applied to the 5m-square-grids bathymetry data around the Tenryu river mouth and the incident wave conditions, H_s=0.8m, T_s=7.8s, and θ=S12^{o}E, were applied for computations of the wave fields at 10:00 on July 28th, when tracing survey of color sands and gravels were carried out. Either regular or unidirectional random waves were applied. In order to investigate the influence of the wave-current interactions, three different river discharge rates, Q=0, 140, and 280m^3/s, were respectively applied at the upstream boundary.

Wave Overtopping around the East Tip of the Spit

Digital snap shot images were firstly analyzed to evaluate the spatial distributions of the inundation rate, the ratio of duration when the area was submerged and the entire observing time. Based on the RGB-values at each pixel of the original snap shot images, we first setup the threshold values which determine whether the pixel is wet or dry. Based on the obtained threshold values, original image was transferred to the binary images with 0 and 1 corresponding to dry and wet, respectively. The same procedures were applied to the 750 succeeding snap shot images, which cover 15-minute-observation period. The inundation rate was computed at each pixel as a ratio of the number of images which was wet at the same pixel out of the total number of images. Finally, obtained images of the inundation rate were rectified to obtain the spatial distributions of the inundation rate based on the geographic XY-coordinate system. Figure 9 shows the obtained horizontal distributions of the inundation rates respectively at 7:00 and 10:00 on July 28th. Figure 9 also

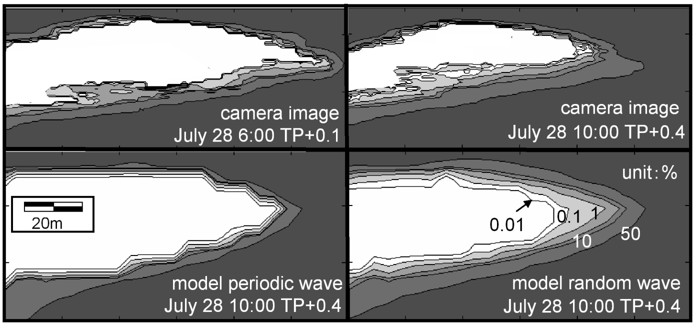

Fig. 9 Horizontal distributions of observed (top two) and predicted (bottom two) inundation rates.

shows the computed inundation rate, based on the same definition used in the image analysis, when either periodic regular or unidirectional random waves were respectively incident. As seen in the top two figures, observed spatial distributions of the inundation rates are highly affected by the tidal water level. Especially around the east end of the spit, where has lower and milder cross-section profiles, increase of the inundated area was more significant. As shown in two bottom panels of Figure 9, numerical model showed reasonable predictive skills of the horizontal distributions of inundation rate when unidirectional random waves were incident. Considering the observed fact that gravels placed around the east end of the spit was transported to the north only when relatively long wave ran up on the spit, it is deduced that randomness of the wave frequency is one of crucial factors to determine the cross-shore movement of the sediment grains on the sand spit.

Wave Directions around the River Mouth

Numerical model was applied for estimation of the alongshore distributions of the wave directions along the depth contour lines at T.P.-1.0m. Figure 10 compares instantaneous surface water profiles when either periodic regular or unidirectional random waves were introduced with or without the river discharge. The river discharge rate, Q=280m^3/s, yielded the observed current velocity, 1.4m/s, at the river mouth where the acoustic Doppler velocity profiler was installed. Besides the instantaneous surface water elevations, indicated in shadings, these figures also show bathymetry used for the wave computation in contour lines. As compared in the first two panels of the Figure 10, the river flow surely has certain impacts on wave refractions and waves appeared to be concentrated more near the east tip of the spit when the river discharge was taken into account.

Figure 11 compares the alongshore distributions of predicted wave directions at 1-meter-deep-contour line, shore-normal directions, and the difference of these two directions. In the figure, P0, P1 and P2 are predictions of regular wave case with Q=0, 140, and 280m^3/s, respectively whereas R2 is predictions with random incident waves with Q=280m^3/s. As seen in the figure, wave directions abruptly changes within the distance of 100m from the east tip of the spit. As seen in comparisons of P0, P1 and P2, river discharge decrease the wave angle within the horizontal range of 500m from the tip. This decrease of the wave angle surely acts to increase eastward movement of the sediments near the tip of the

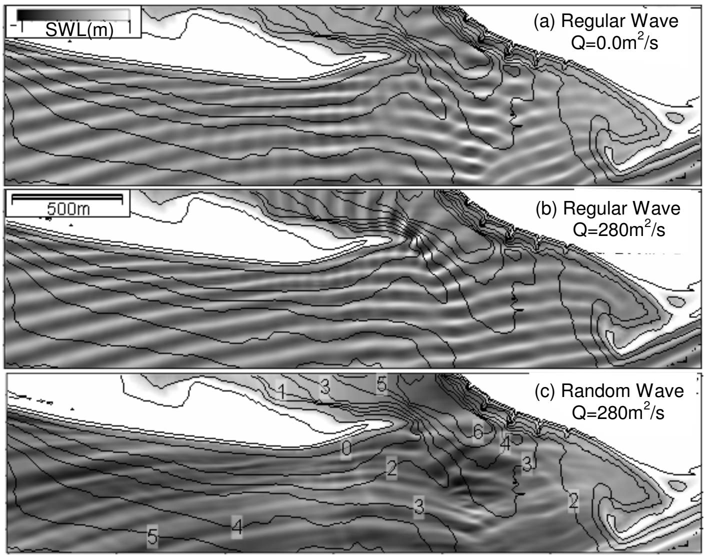

Fig. 10 Comparisons of predicted instantaneous surface water profiles.

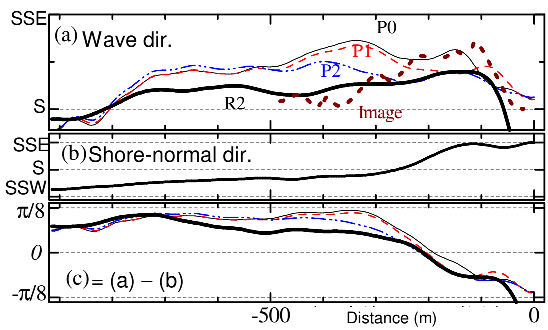

Fig. 11 Alongshore distributions of (a) wave directions, (b) shore-normal directions, and (c) difference between (a) and (b). Distance is from the east tip of the spit. (positive in eastward) P1, P2 and P3 denote the regular incident wave cases with Q=0, 140, and 280m^3/s, respectively whereas R2 denotes the unidirectional random wave case with Q=280m^3/s.

spit. It is also seen that the random waves tend to be refracted more due to the presence of lower frequency wave components.

Conclusion

Based on the unique set of field survey, this study aimed to investigate the movement of sand and gravels and resulting deformations of the sand spit at the Tenryu river mouth.

Daily deformation of the east tip of the sand spit was first analyzed based on the succeeding snap shot images recorded by field cameras. Relatively large river flow eroded only the north-east side of the sand spit. Relatively large waves overtopped the east end of the spit and moved it landward. Moderate waves following the stormy waves transported offshore sediments shoreward and increased the land area only around the seaside of the sand spit. Significant morphology change showed clear correlation with spring tide. Even when the waves were incident from the south-east, sand spit was fairy stable.

Color sand and gravels were placed at the outer edge of the swash zone of both west and east sides of the sand spit and their spatial distributions were traced. Sands and gravels placed on each side of the spit moved toward the opposite alongshore directions. Especially at the east tip of the spit, gravels tended to move in the cross-shore northward direction rather than the alongshore eastward directions whereas sand moved north-east directions.

Finally, hydrodynamic characteristics were investigated through the analysis of obtained images as well as the numerical analysis especially focusing on wave overtopping on the spit and alongshore distributions of the wave angle against shore-normal direction. Wave overtopping was strongly affected by tidal water level as well as randomness of the incident waves. River discharge affected to change the wave directions around the river mouth and induced the sediment in the direction to which the sand spit was extended. All of these findings, based on images, hydrodynamics, tracer surveys and numerical analysis, were consistent and supported with each other.

Acknowledgements

Authors sincerely acknowledge that this study is a part of Tenryu-Enshunada Project financially supported by the Japan Science and Technology Agency (JST).

References

Bell, P.S. (1999). “Shallow water bathymetry derived from an analysis of X-band marine radar images of waves,” *Coastal Eng.*, 37, 451-523.

Greidanus, H. (1997). “The use of radar for bathymetry in shallow seas,” *Hydrographic J.*, 83, 13-18.

Lippmann, T.C., and R.A. Holman (1989). “Quantification of sand bar morphology: A video technique based on wave dissipation,” *J. Geophys. Res*. 94(C1), 995-1011.

Liu, H., Tajima, Y. and Sato, S. (2009). “Field study on the nearshore sediment process around the Tenryu estuary using image analysis,” *Proc. of Int. Conf. on Coastal Dynamics*, .

Niu, X., Ueyama, S., Sato, S., Tajima, Y., and Liu, H. (2009). “Sediment movement under combined waves, tide and river discharge in a river mouth,” *Proc. of Int. Conf. on Coastal Dynamics*, .

Madsen, P.A., Sorensen, O.R. and Schaffer, H.A.(1997). “Surf zone dynamics simulated by a Boussinesq type model. Part I. Model description and cross-shore motion of regular waves,” *Coast. Eng.*, 32, Elsevier, 255-287

Tajima, Y., Liu, H., and Sato S. (2009). “Dynamic changes of waves and currents over the collapsing sandbar of the Tenryu river mouth observed during typhoon T0704,” *Proc. of Int. Conf. on Coastal Dynamics*, .

Tajima, Y., Sato, S., Shimozono, T. and M. Isobe. (2007). “Characteristics and modeling of wave-induced current around submerged detached breakwaters,” *Int. Conf. on Coastal Structures*, CD-ROM.

Takagawa, T., Tajima, Y., Liu, H, Takewaka, S., and Sato, S. (2011). “Dynamic topography changes of sand spit of the Tenryu river mouth due to overtopping waves,” *Int. Conf. on Coastal Sediments*